Sci. Bull. (2015) 60(22):1954–1961
DOI 10.1007/s11434-015-0917-6

CrossMark

www.scibull.com
www.springer.com/scp

Article

Earth Sciences

Optimizing photosynthetic and respiratory parameters based on the seasonal variation pattern in regional net ecosystem productivity obtained from atmospheric inversion

Zhuoqi Chen · Jing M. Chen · Xiaogu Zheng · Fei Jiang · Jun Qin · Shupeng Zhang · Wenping Yuan · Weiming Ju · Gang Mo

Received: 30 July 2015 / Accepted: 29 September 2015 / Published online: 22 October 2015

Abstracts In this study, we explore the feasibility of optimizing ecosystem photosynthetic and respiratory parameters from the seasonal variation of the net carbon flux. An optimization scheme is proposed to estimate two key parameters ($V_{\max}^{25}$ and Q_{10}) by exploiting the seasonal variation in the net ecosystem carbon flux retrieved by an atmospheric inversion system. This scheme is implemented to estimate $V_{\max}^{25}$ and Q_{10} of the boreal ecosystem productivity simulator (BEPS) to improve its NEP simulation in the boreal North American region. Then, in situ NEE observations at six eddy covariance sites are used to evaluate the NEE simulations from BEPS with initial and optimized parameters. The results show that the performance of the optimized BEPS is superior to that of the BEPS with the default parameter values. These results implicate that it is possible to optimize ecosystem model parameters by different sensitivities of $V_{\max}^{25}$ and Q_{10} during growing and non-growing seasons through atmospheric inversion or data assimilation techniques.

Keywords Parameter optimization · Land surface model · CO_2 concentration measurements · NEP

1 Introduction

Ecological models integrate principal processes and mechanisms that relate to energy partitioning and carbon uptake. They have been extensively used in ecological research for simulating ecosystem productivity, greenhouse gas emission, and water consumption. Since the developments of ecological models in the 1960s [1, 2], they have been continuously improved to match with new observations [3]. Uncertainties of parameters in these models are identified as a major source of model errors [4, 5]. Various methods and eddy covariance (EC) measurements have been used for parameter estimation in these models [6–12]. However, due to different spatial scales and environment factors, parameters best fit to EC measurements at sites may not best represent the average conditions of a region. It is, therefore, often necessary to recalibrate these parameters for different sites and different times. For regional applications, it is highly desirable to derive parameters of ecological models that represent the regional average conditions.

Atmospheric inversion (AI) techniques were widely used to estimate land and ocean carbon fluxes based on atmospheric CO_2 measurements [13–19]. Since atmospheric CO_2 measurements are intrinsically influenced by regional ecosystem carbon fluxes, carbon fluxes derived from AI systems can allow us to obtain parameters of ecological models applicable at the regional scale [20–24]. Because photosynthetic and respiratory processes simultaneously contribute to the net ecosystem carbon flux [25], it is generally perceived to be difficult to separate the net flux

Z. Chen · X. Zheng · S. Zhang · W. Yuan
College of Global Change and Earth System Science, Beijing Normal University, Beijing 100875, China

J. M. Chen · F. Jiang · W. Ju
International Institute for Earth System Science, Nanjing University, Nanjing 210023, China

J. M. Chen (✉) · G. Mo
Department of Geography and Program in Planning, University of Toronto, Toronto, Ontario M5S 2E8, Canada
e-mail: jing.chen@utoronto.ca

J. Qin
Key Laboratory of Tibetan Environment Changes and Land Surface Processes, Institute of Tibetan Plateau Research, Chinese Academy of Sciences, Beijing 100101, China

into photosynthesis and respiration components without any additional information [26, 27]. However, this perception may be challenged by utilizing a data assimilation technique. Addressing this challenge has profound implications on the feasibility of using atmospheric CO_2 concentration measurements for optimizing ecosystem parameters, which has been done by CCDAS [20–24]. In this study, we try to optimize ecosystem model parameters by exploring different sensitivities of $V_{\max}^{25}$ and Q_{10} during growing and non-growing seasons through data assimilation techniques.

The objectives of this study are (1) to explore ways to use ecosystem carbon fluxes derived from an AI system for estimating parameters of an ecological model for regional applications and (2) to investigate the possibility of estimating photosynthetic and respiratory parameters from the seasonal variation pattern of ecosystem carbon fluxes.

2 Data and method

2.1 Data sources

Ecosystem carbon fluxes for boreal North America boreal (BNA) region obtained from an atmospheric inversion (AI) system [16] are used to optimize parameters in the BEPS model from 2003 to 2008. Measurements of net ecosystem exchange (NEE), which is opposite in sign to net ecosystem productivity (NEP), from 6 EC sites, are used to evaluate the success of our optimization scheme through comparing NEP simulations from BEPS with initial and optimized parameters. The EC sites are CA-Gro [28], CA-Mer [29], CA-Oas [30], CA-Obs [31], CA-TP4 [32], and CA-WP1 [33]. All these 6 sites are selected to evaluate terrestrial biosphere models in North American Carbon Program [34].

2.2 Model description

The boreal ecosystem productivity simulator model (BEPS) [35, 36] is used for simulating NEP of terrestrial ecosystems at 1° resolution. Each grid cell can be made up of any mixture of seven plant functional types (PFT) [37]. In this model, canopy photosynthesis is estimated using the biochemical Farquhar's model [38] coupled with a stomatal conductance model [39, 40]. The canopy-level mean maximum carboxylation rate at 25 °C ($V_{\max,j}^{25}$, j is a specific PFT type) is a key parameter for canopy photosynthesis. Since there are seven PFTs in every 1° grid cell, it is hard to trace the variation of $V_{\max,j}^{25}$ for every PFT. Therefore, as an alternative, it is assumed that the $V_{\max,j}^{25}$ of all PFTs change with the same proportion. $V_{\max,j}^{25}$ can be expressed as follows:

$$V_{\max,j}^{25} = \beta \times V_{\max}^{25}, \tag{1}$$

where $V_{\max}^{25}$ is a base maximum carboxylation rate for all PFTs, which is equal to 50 μmol m^{-2} s^{-1}. β is a multiplier and kept constant in optimization process. In this study, we optimize the base maximum carboxylation rate ($V_{\max}^{25}$) for all PFTs.

Soil respiration is modeled as a function of temperature with the widely used Q_{10} function (Eq. 2).

$$SR = r_b \times Q_{10}^{\frac{T_s-10}{10}}, \tag{2}$$

where SR is soil respiration, r_b is base respiration rate related to carbon pools at the reference temperature, and T_s is soil temperature. Q_{10} is another key parameter for soil respiration. Default value for Q_{10} is 2.3.

2.3 Basis of optimization scheme

It is difficult to estimate parameter values for respiration and photosynthesis together by using NEP measurements at a given time without additional information. However, the seasonal variation pattern of NEP data may be utilized for providing additional information to estimate parameter values for respiration and photosynthesis together. A sensitivity analysis of parameters (Fig. 1a) in BEPS indicates that changes in $V_{\max}^{25}$ contribute more to changes in NEP in the growing season (from May to August), while Q_{10} affects NEP in the non-growing/transition season (from September to April) at CA-Obs site. Gross primary productivity (GPP) is close to zero during the non-growing season (from November to March, Fig. 1b), while soil respiration dominates the ecosystem carbon flux during this period. During the growing season, changes in soil respiration induced by changes in Q_{10} are small (Fig. 1c) since the average soil temperature ranges from 8 to 12 °C during this season. Photosynthesis therefore contributes more to ecosystem carbon fluxes than soil respiration during this period. The seasonal variation pattern of NEP contains, to a large extent, separate information for photosynthetic and respiratory parameters.

Since photosynthesis is weak during non-growing and transition seasons, soil respiration and Q_{10} values can be estimated from NEP. Because of seasonal variations in Q_{10} [41], Q_{10} values estimated during the non-growing season cannot be used for the growing season. Therefore, annual cumulative NEP measurements are used to determine $V_{\max}^{25}$, while seasonal variations in NEP are used to optimize Q_{10}.

2.4 Optimization scheme

For the BNA region, we assume the period from May to August to be the growing season. Other months are in non-growing/transition seasons. Q_{10} is estimated every 4 months (January–April, May–August, and September–December), and $V_{\max}^{25}$ is estimated once a year. Based on the Bayesian

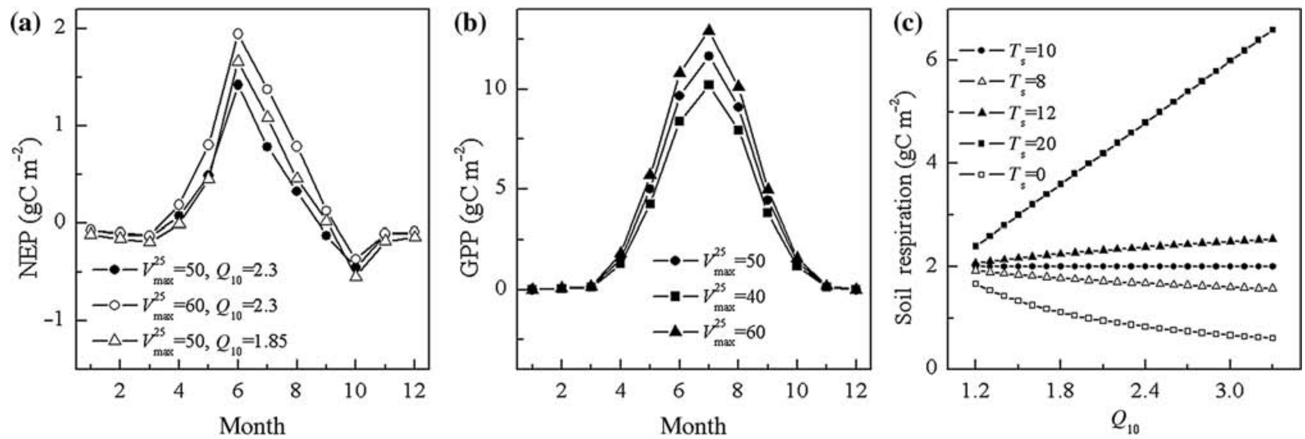

Fig. 1 Sensitivity analyses of respiratory and photosynthesis parameters in the BEPS model at the CA-Obs site. **a** NEP simulated by BEPS with different $V_{\max}^{25}$ and Q_{10}, **b** GPP simulated by BEPS with different $V_{\max}^{25}$, **c** Soil respiration simulated by BEPS with different Q_{10} and soil temperature (T_s)

theory, the cost function (Eq. 3) is used to find the maximum likelihood solution of the variables x as a balance between observations and prior knowledge given by the model.

$$J(x) = \frac{1}{2}(x - x_b)^{\mathrm{T}} B^{-1}(x - x_b) + \frac{1}{2}(BEPS(x) - NEP_{\mathrm{AI}})^{\mathrm{T}}(O + P)^{-1}(BEPS(x) - NEP_{\mathrm{AI}}), \quad (3)$$

where x and x_b are scalars containing optimized and default parameters in BEPS, respectively. $BEPS(x)$ is regarded as a nonlinear operator which is used to estimate ecosystem carbon fluxes with corresponding parameter x. $\mathrm{NEP_{AI}}$ is ecosystem carbon fluxes from measurements or derived from an AI system. O is a posterior error covariance of $\mathrm{NEP_{AI}}$ from the AI system. B is the error covariance matrix of default parameters. We assume that errors of Q_{10} and $V_{\max}^{25}$ are statistically independent. P is the error covariance matrix of BEPS. We estimate P by using a perturbed ensemble of model parameters x. An inflation approach [42] on the error covariance matrix is used to estimate B and P. We follow the Ensemble Kalman filter (EnKF) framework [43] to estimate model parameters. Since $BEPS(x)$ is nonlinear and complicated, linearized approximation in EnKF may not find the best parameters. Therefore, a global optimization method called SCE-UA [44] is employed to minimize the cost function.

In order to save time spent on minimizing the cost function, we design a optimization scheme, called multi-timescale scheme, to estimate $V_{\max}^{25}$ and Q_{10} values step by step. There are four steps in the optimization scheme. In the first step, the initial soil carbon pools are obtained through a long-term spin-up process [45]. As the size of carbon pools in the soil changes little over a short period of time, they are kept constant in the following optimization. The optimization steps use the same cost function (Eq. 3) but with different x, x_b, B, and P. In the second step, $V_{\max}^{25}$ is estimated once a year. In the cost function, x is $V_{\max}^{25}$. Q_{10} is kept at the prior value in the BEPS model. In the third step, Q_{10} is determined every four months. In the cost function, x is Q_{10}. $V_{\max}^{25}$ is the estimated value from previous step. In the last step, optimized $V_{\max}^{25}$ and Q_{10} are compared to the prior parameters in the model. If the difference between prior and optimized parameter values is less than 1 for $V_{\max}^{25}$ and 0.1 for Q_{10}, the process of optimization is completed. If not, steps 2 and 3 will be repeated using optimized parameters as prior parameters.

3 Results and discussion

The multi-timescale optimization scheme described above is first applied to flux data at the CA-Obs site to demonstrate the methodology for optimizing $V_{\max}^{25}$ and Q_{10} at the site level. The scheme is then used for optimizing $V_{\max}^{25}$ and Q_{10} to the regional NEP obtained from AI for the purpose of exploring the feasibility of using atmospheric CO_2 concentration measurements for optimizing ecosystem parameters.

At the CA-Obs site, NEP simulated by BEPS with default parameters is larger in the non-growing/transition season and smaller in the growing season than in observations (Fig. 2a). To show the effectiveness of the multi-timescale optimization scheme, three optimization schemes are designed to compare with each other. The same cost function (Eq. 3) is used in all schemes. Only $V_{\max}^{25}$ (Q_{10}) is estimated in Scheme I (Scheme II). These two schemes do not use the information hidden in multi-timescale NEP data. Both $V_{\max}^{25}$ and Q_{10} are estimated in Scheme III (multi-timescale optimization scheme). NEP simulated by BEPS with optimized $V_{\max}^{25}$ or Q_{10} through Schemes I and II

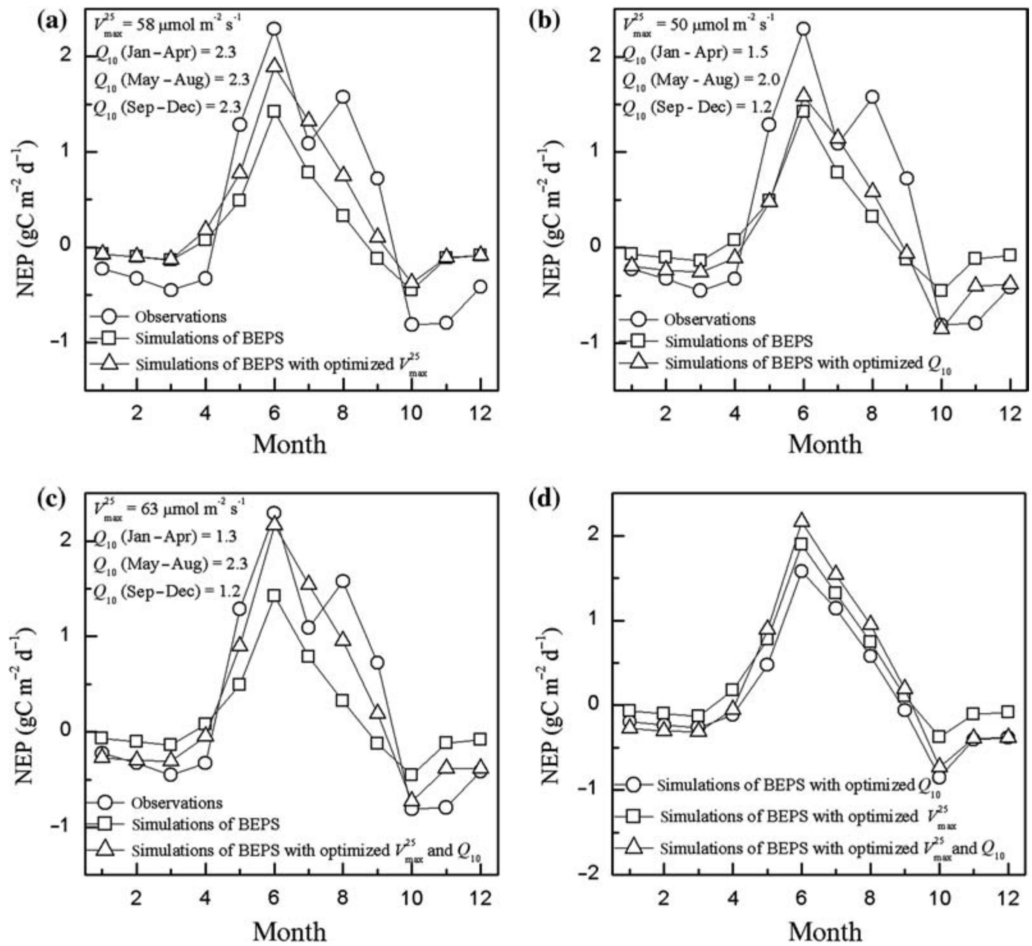

Fig. 2 Result of NEP simulations by BEPS with parameters estimated by different optimization schemes at CA-Obs site in 2004. **a** Result of NEP simulations by BEPS with optimized V_{max}^{25} (Scheme I), **b** Result of NEP simulations by BEPS with optimized Q_{10} (Scheme II), **c** Result of NEP simulations by BEPS with optimized V_{max}^{25} and Q_{10} (multi-timescale Scheme), **d** Comparisons between NEP simulations by BEPS with parameters estimated by different schemes

(Fig. 2a, b) is closer to observations than NEP simulated by BEPS with default parameters. NEP simulated by BEPS with optimized V_{max}^{25} (Q_{10}) follows observations well in the growing season (non-growing/transition season). But NEP simulations are little improved in the non-growing/transition season (growing season). These results suggest that both photosynthetic and respiratory parameters are responsible for the discrepancy between the prior and observed NEP.

The multi-timescale optimization scheme is used to estimate V_{max}^{25} and Q_{10}. NEP simulations by BEPS with optimized V_{max}^{25} and Q_{10} through Scheme III follow NEP measurements well throughout the year (Fig. 2c). Estimated parameters for every step are listed in Table 1. V_{max}^{25} is firstly estimated to be 58 μmol m^{-2} s^{-1}, which is a little higher than the default value. NEP simulations by BEPS with optimized V_{max}^{25}, which is similar to that used in Scheme I (Fig. 1a), are close to measurements in the growing season and the measured total annual accumulative NEP. However, the performance of BEPS with new V_{max}^{25} is not improved during the non-growing/transition season. In the next step, Q_{10} is estimated to be in the range from 1.4 to 1.2 in non-growing/transition season and from 2.3 to 2.2 in the growing season. NEP simulations by BEPS with optimized Q_{10}, which is similar to that used in Scheme II (Fig. 2b), are close to measurements in the non-growing/transition season. Since NEP simulations are reduced with the optimized Q_{10} in the non-growing/transition season, the simulated annual total NEP would deviate from measurements again after this step. Then V_{max}^{25} is optimized for the second time. These two steps iterate until V_{max}^{25} and Q_{10} are both convergent (invariant). It takes 4 iterations to achieve the convergence. Optimized V_{max}^{25} is 63 μmol m^{-2} s^{-1}, and optimized Q_{10} is 1.3 (1.2) and 2.3 in the non-growing/transition and the growing season, respectively. Optimized Q_{10} is equal to the default value in BEPS in the growing season. This result indicates that the discrepancy between simulations and measurements is only used to

Table 1 Parameters estimated in each step at the CA-Obs site

	Default	V^{1st}	Q^{1st}	V^{2nd}	Q^{2nd}	V^{3rd}	Q^{3rd}	V^{4th}
Estimated V_{cmax} first								
V_{cmax}	50	58	58	60	60	63	63	63
Q_{10} (Jan–Apr)	2.3	2.3	1.4	1.4	1.2	1.2	1.3	1.3
Q_{10} (May–Aug)	2.3	2.3	2.2	2.2	2.2	2.2	2.3	2.3
Q_{10} (Sep–Dec)	2.3	2.3	1.2	1.2	1.2	1.2	1.2	1.2
	Default	Q^{1st}	V^{1st}	Q^{2nd}	V^{2nd}	Q^{3rd}	V^{3rd}	Q^{4th}
Estimated Q_{10} first								
V_{cmax}	50	50	55	55	59	59	63	63
$Q_{10}^{(Jan–Apr)}$	2.3	1.5	1.5	1.3	1.3	1.2	1.2	1.3
$Q_{10}^{(May–Aug)}$	2.3	2.0	2.0	2.0	2.0	2.2	2.2	2.3
$Q_{10}^{(Sep–Dec)}$	2.3	1.2	1.2	1.2	1.2	1.2	1.2	1.2

Unit of V_{max}^{25} is μmol m^{-2} s^{-1}; Q_{10} is dimensionless. Character "V" means V_{max}^{25} is estimated in this step. Character "Q" means Q_{10} is estimated in this step. Superscripts of character "V" or "Q" stand for iterative times

optimize V_{max}^{25} in the growing season. As shown in Fig. 2d, optimized V_{max}^{25} tends to make NEP simulations increase in the growing season. In contrast, decreased Q_{10} tends to make NEP simulations decrease in the non-growing /transition season. We design an alternative scheme to estimate V_{max}^{25} and Q_{10} again. In this scheme, we change the optimization order of V_{max}^{25} and $Q_{10,}$ i.e., Q_{10} is estimated first and then V_{max}^{25}. The results of the alternative scheme are the same as Scheme III (Table 1). All these results indicate that the multi-timescale NEP data can be used to estimate two key parameters (V_{max}^{25} and Q_{10}) for ecological models.

The same multi-timescale scheme is subsequently used to estimate V_{max}^{25} and Q_{10} using NEP derived from an AI system [16] as measurements in BNA region. Estimated V_{max}^{25} ranges from 49 to 57 μmol m^{-2} s^{-1} (Table 2). Based on results of Kattge et al. [46], BEPS assigns V_{max}^{25} for each plant functional types (PFT) [37]. Broadleaf deciduous and coniferous deciduous forests are the most dominant PFTs in BNA. The V_{max}^{25} for these two PFTs are 57.7 ± 21.2 and 39.1 ± 11.7 μmol m^{-2} s^{-1}, respectively. The optimized V_{max}^{25} falls between these values. Conventional estimates based on observation data suggest that Q_{10} ranged from 1 to 4.2 [47, 48]. Estimated Q_{10} ranges from 1.6 to 2.2 during both the growing season and the non-growing/transition season (Table 2). As shown in Fig. 3, NEP derived from the AI system is larger (lower) than that from BEPS with default parameters (BEPS-P) in the growing (non-growing/transition) season. Optimized NEP falls between AI and BEPS models' output at most times. Annual accumulative NEP from the AI system, BEPS-P, and BEPS with optimized parameters (BEPS-O) is 0.28, 0.02 and 0.11 PgC/yr, respectively, during 2003–2008 in BNA. The North American Carbon Program indicated that NEP simulations from several ecological models varied between −0.2 and 0.7 PgC/yr in the BNA [49]. NEP from AI, BEPS-P, and BEPS-O are all in this range. But NEP from BEPS-O is closer to the mean value of all ecological models, which is 0.1 PgC/yr, than the other estimates. NEE based on EC measurements from six flux sites are used to evaluate outputs of BEPS-P and BEPS-O. These EC sites spanned 4 PFTs and were uniformly distributed in BNA. The regional V_{max}^{25} is not suited to simulate NEP for a specific PFT. V_{max}^{25} for each FT is calculated by using estimated regional V_{max}^{25} and the ratios between regional V_{max}^{25} and V_{max}^{25} for each PFT (described in Sect. 2.2). Then BEPS model can be used to simulate NEP with new parameters at these EC sites. As shown in Fig. 4, BEPS-O outperforms BEPS-P at all sites. It is noted that the R^2 values for some sites are low for BEPS-O because regionally optimized V_{max}^{25} and Q_{10} are used, which are only a first approximation.

Table 2 Parameters estimated using atmospherically inverted net primary productivity for boreal North America

	Prior	2003	2004	2005	2006	2007	2008
V_{cmax} at 25 °C	50	55	50	56	49	57	50
Q_{10} (Jan–Apr)	2.3	1.9	1.8	1.8	1.8	1.8	1.7
Q_{10} (May–Aug)	2.3	2.1	2.1	2.2	2.2	2.1	2.2
Q_{10} (Sep–Dec)	2.3	2.0	2.0	2.0	1.6	1.8	2.0

Unit of V_{max}^{25} is μmol m^{-2} s^{-1}; Q_{10} is dimensionless

We proposed a scheme to estimate parameters in BEPS by using CO_2 flux from an atmospheric inversion system. Several similar studies have been done in recent years [20–24]. The main challenge facing these studies is how to estimate photosynthetic and respiratory parameters by using only data of NEP which is a balance between photosynthetic and respiration processes. For instance, if a

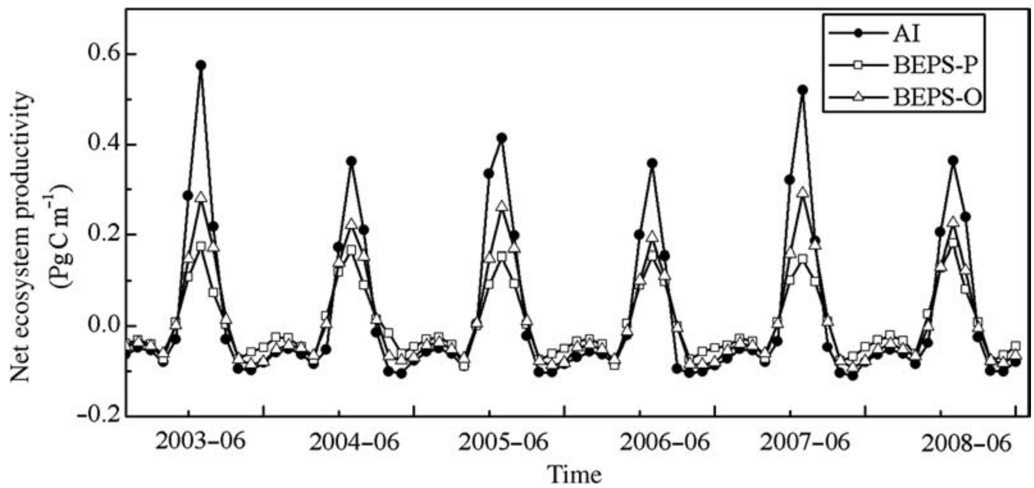

Fig. 3 NEP from atmospheric inversion, the BEPS model with default parameters and the BEPS model with optimized parameters in boreal North America during 2003–2008

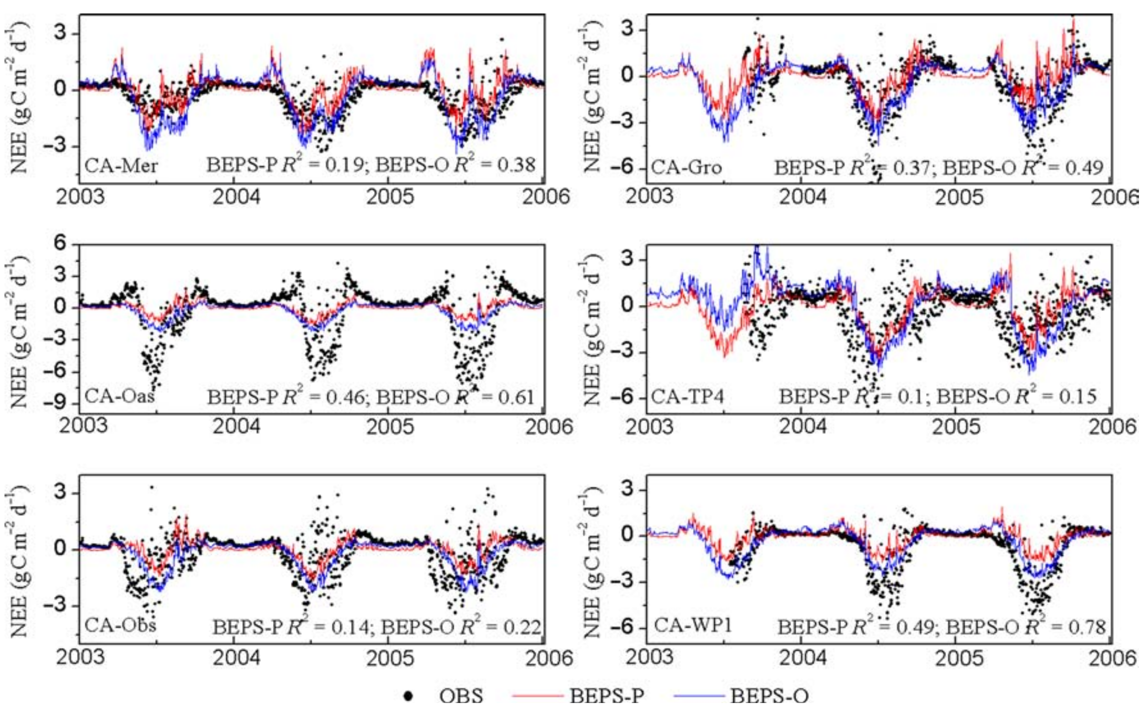

Fig. 4 Comparisons between NEE measurements, NEE simulations from BEPS with default parameters values and with optimized parameters values at six flux sites in boreal North America

model overestimates NEP, this model error can be corrected via only adjusting photosynthetic or respiration parameters. In previous studies [20–24], optimized parameters depend on predefined uncertainties of these parameters. For example, if uncertainties of respiration parameters are larger than those of photosynthetic parameters, respiration parameters tend to be changed more than photosynthetic parameters. The difference between our and other schemes is that our scheme makes use of the different sensitivities of $V_{\max}^{25}$ and Q_{10} during growing and non-growing seasons to optimize photosynthetic and respiratory parameters simultaneously.

4 Conclusion

In this study, a multi-timescale optimization scheme is proposed to estimate two key parameters ($V_{\max}^{25}$ and Q_{10}) in BEPS for regional applications. The following conclusions are drawn from this study:

1. For the boreal North America, where photosynthesis and respiration contribute differently to the net ecosystem productivity in different seasons, it is feasible to optimize both photosynthesis (V_{max}^{25}) and respiratory (Q_{10}) parameters. We found that V_{max}^{25} is sensitive to NEP in the growing season, while Q_{10} can be optimized in the non-growing and transitional seasons as well as in the growing season.
2. In the growing season, both V_{max}^{25} and Q_{10} control NEP, and both parameters can be optimized. It makes little difference which parameter is optimized first. This is probably due to the fact that V_{max}^{25} determines the overall magnitude of the NEP, while Q_{10} influences more the temporal pattern of NEP with temperature than the overall magnitude.
3. Regional ecosystem carbon fluxes derived from AI systems can allow us to obtain parameters of ecological models applicable at the regional scale. However, it is difficult to prove that the performance of BEPS with optimized parameters is better than that of BEPS with default parameters at regional scale. Comparing to measurements from EC sites, NEP simulations from the optimized BEPS model are better than the simulations from the BEPS model with default parameter values over four different PFTs.

Acknowledgments This work was supported by the National Basic Research Program of China (2010CB950703) and the National Natural Science Foundation of China (41571338).

Conflict of interest The authors declare that they have no conflict of interest.

References

1. Odum HT (1956) Primary production in flowing waters. Limnol Oceanogr 1:102–117
2. Watt KE (1967) Systems analysis in ecology. Academic Press, New York
3. Wang YP, Trudinger CM, Enting IG (2009) A review of applications of model-data fusion to studies of terrestrial carbon fluxes at different scales. Agric Forest Meteorol 149:1829–1842
4. Green EJ, MacFarlane DW, Valentine HT et al (1999) Assessing uncertainty in a stand growth model by Bayesian synthesis. Forest Sci 45:528–538
5. Luo YQ, White LW, Canadell JG et al (2003) Sustainability of terrestrial carbon sequestration: a case study in Duke Forest with inversion approach. Glob Biogeochem Cycle. doi:10.1029/2002GB001923
6. Braswell BH, Sacks WJ, Linder E et al (2005) Estimating diurnal to annual ecosystem parameters by synthesis of a carbon flux model with eddy covariance net ecosystem exchange observations. Glob Change Biol 11:335–355
7. Gove J, Hollinger D (2006) Application of a dual unscented Kalman filter for simultaneous state and parameter estimation in problems of surface-atmosphere exchange. J Geophys Res. doi:10.1029/2005JD006021
8. Knorr W, Kattge J (2005) Inversion of terrestrial ecosystem model parameter values against eddy covariance measurements by Monte Carlo sampling. Glob Change Biol 11:1333–1351
9. Mo X, Chen JM, Ju W et al (2008) Optimization of ecosystem model parameters through assimilating eddy covariance flux data with an ensemble Kalman filter. Ecol Model 217:157–173
10. Wang YP, Leuning R, Cleugh HA et al (2001) Parameter estimation in surface exchange models using nonlinear inversion: how many parameters can we estimate and which measurements are most useful? Glob Change Biol 7:495–510
11. Williams M, Schwarz PA, Law BE et al (2005) An improved analysis of forest carbon dynamics using data assimilation. Glob Change Biol 11:89–105
12. Yuan W, Liang S, Liu S et al (2012) Improving model parameter estimation using coupling relationships between vegetation production and ecosystem respiration. Ecol Model 240:29–40
13. Ciais P, Peylin P, Bousquet P (2000) Regional biospheric carbon fluxes as inferred from atmospheric CO_2 measurements. Ecol Appl 10:1574–1589
14. Deng F, Chen JM, Ishizawa M et al (2007) Global monthly CO_2 flux inversion with a focus over North America. Tellus B 59:179–190
15. Gurney KR, Law RM, Denning AS et al (2002) Towards robust regional estimates of CO_2 sources and sinks using atmospheric transport models. Nature 415:626–630
16. Jiang F, Wang H, Chen J et al (2013) Nested atmospheric inversion for the terrestrial carbon sources and sinks in China. Biogeosciences 10:5311–5324
17. Peters W, Krol M, Van Der Werf G et al (2010) Seven years of recent European net terrestrial carbon dioxide exchange constrained by atmospheric observations. Glob Change Biol 16:1317–1337
18. Peylin P, Rayner P, Bousquet P et al (2005) Daily CO_2 flux estimates over Europe from continuous atmospheric measurements: 1, inverse methodology. Atmos Chem Phys 5:3173–3186
19. Rayner P, Law R, Allison C et al (2008) Interannual variability of the global carbon cycle (1992–2005) inferred by inversion of atmospheric CO_2 and $\delta^{13}CO_2$ measurements. Glob Biogeochem Cycle. doi:10.1029/2007GB003068
20. Kaminski T, Knorr W, Rayner PJ et al (2002) Assimilating atmospheric data into a terrestrial biosphere model: a case study of the seasonal cycle. Glob Biogeochem Cycle. doi:10.1029/2001GB001463
21. Koffi EN, Rayner PJ, Scholze M et al (2012) Atmospheric constraints on gross primary productivity and net ecosystem productivity: results from a carbon-cycle data assimilation system. Glob Biogeochem Cycle. doi:10.1029/2010GB003900
22. Koffi EN, Rayner PJ, Scholze M et al (2013) Quantifying the constraint of biospheric process parameters by CO_2 concentration and flux measurement networks through a carbon cycle data assimilation system. Atmos Chem Phys 13:10555–10572
23. Rayner PJ, Scholze M, Knorr W et al (2005) Two decades of terrestrial carbon fluxes from a carbon cycle data assimilation system (CCDAS). Glob Biogeochem Cycle. doi:10.1029/2004GB002254
24. Ziehn T, Knorr W, Scholze M (2011) Investigating spatial differentiation of model parameters in a carbon cycle data assimilation system. Glob Biogeochem Cycle. doi:10.1029/2010GB003886
25. Wang QF, Zheng H, Zhu XJ et al (2015) Primary estimation of Chinese terrestrial carbon sequestration during 2001–2010. Sci Bull 60:577–590
26. Lasslop G, Reichstein M, Papale D et al (2010) Separation of net ecosystem exchange into assimilation and respiration using a light response curve approach: critical issues and global evaluation. Glob Change Biol 16:187–208
27. Reichstein M, Falge E, Baldocchi D et al (2005) On the separation of net ecosystem exchange into assimilation and ecosystem

respiration: review and improved algorithm. Glob Change Biol 11:1424–1439
28. McCaughey J, Pejam M, Arain M et al (2006) Carbon dioxide and energy fluxes from a boreal mixedwood forest ecosystem in Ontario, Canada. Agric For Meteorol 140:79–96
29. Lafleur PM, Roulet NT, Bubier JL et al (2003) Interannual variability in the peatland-atmosphere carbon dioxide exchange at an ombrotrophic bog. Glob Biogeochem Cycle 17:1036
30. Barr AG, Black T, Hogg E et al (2004) Inter-annual variability in the leaf area index of a boreal aspen-hazelnut forest in relation to net ecosystem production. Agric For Meteorol 126:237–255
31. Griffis T, Black T, Morgenstern K et al (2003) Ecophysiological controls on the carbon balances of three southern boreal forests. Agric For Meteorol 117:53–71
32. Peichl M, Arain MA (2007) Allometry and partitioning of above- and belowground tree biomass in an age-sequence of white pine forests. Forest Ecol Manag 253:68–80
33. Syed KH, Flanagan LB, Carlson PJ et al (2006) Environmental control of net ecosystem CO_2 exchange in a treed, moderately rich fen in northern Alberta. Agric For Meteorol 140:97–114
34. Schwalm CR, Williams CA, Schaefer K et al (2010) A model-data intercomparison of CO_2 exchange across North America: results from the North American Carbon Program site synthesis. J Geophys Res. doi:10.1029/2009JG001229
35. Chen J, Liu J, Cihlar J et al (1999) Daily canopy photosynthesis model through temporal and spatial scaling for remote sensing applications. Ecol Model 124:99–119
36. Ju W, Chen JM, Black TA et al (2006) Modelling multi-year coupled carbon and water fluxes in a boreal aspen forest. Agric For Meteorol 140:136–151
37. Chen JM, Mo G, Pisek J et al (2012) Effects of foliage clumping on the estimation of global terrestrial gross primary productivity. Glob Biogeochem Cycle. doi:10.1029/2010GB003996
38. Farquhar G, von Caemmerer S, Berry J (1980) A biochemical model of photosynthetic CO_2 assimilation in leaves of C_3 species. Planta 149:78–90
39. Ball JT (1988) An analysis of stomatal conductance. Thesis, Stanford University Stanford
40. Collatz GJ, Ball JT, Grivet C et al (1991) Physiological and environmental regulation of stomatal conductance, photosynthesis and transpiration: a model that includes a laminar boundary layer. Agric For Meteorol 54:107–136
41. Lloyd J, Taylor J (1994) On the temperature dependence of soil respiration. Funct Ecol 8:315–323
42. Liang X, Zheng X, Zhang S et al (2012) Maximum likelihood estimation of inflation factors on error covariance matrices for ensemble Kalman filter assimilation. Q J R Meteorol Soc 138:263–273
43. Evensen G (2003) The ensemble Kalman filter: theoretical formulation and practical implementation. Ocean Dyn 53:343–367
44. Duan QY, Sorooshian S, Gupta VK (1994) Optimal use of the SCE-UA global optimization method for calibrating watershed models. J Hydrol 158:265–284
45. Chen JM, Ju WM, Cihlar J et al (2003) Spatial distribution of carbon sources and sinks in Canada's forests. Tellus B 55:622–641
46. Kattge J, Knorr W, Raddatz T et al (2009) Quantifying photosynthetic capacity and its relationship to leaf nitrogen content for global-scale terrestrial biosphere models. Glob Change Biol 15:976–991
47. Mahecha MD, Reichstein M, Carvalhais N et al (2010) Global convergence in the temperature sensitivity of respiration at ecosystem level. Science 329:838–840
48. Raich J, Schlesinger WH (1992) The global carbon dioxide flux in soil respiration and its relationship to vegetation and climate. Tellus B 44:81–99
49. Huntzinger D, Post WM, Wei Y et al (2012) North American Carbon Program (NACP) regional interim synthesis: terrestrial biospheric model intercomparison. Ecol Model 232:144–157